AD-A115 098 VIRGINIA UNIV CHARLOTTESVILLE SCHOOL OF ENGINEERING--ETC F/G 11/4
STRUCTURAL CHARACTERIZATION OF SCHLADITZ WHISKERS.(U)
MAY 82 H G WILSDORF N00014-75-C-0691
UNCLASSIFIED UVA/525321/MS82/104 NL

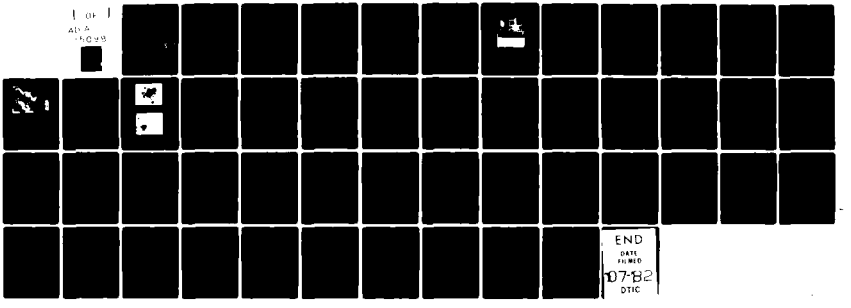

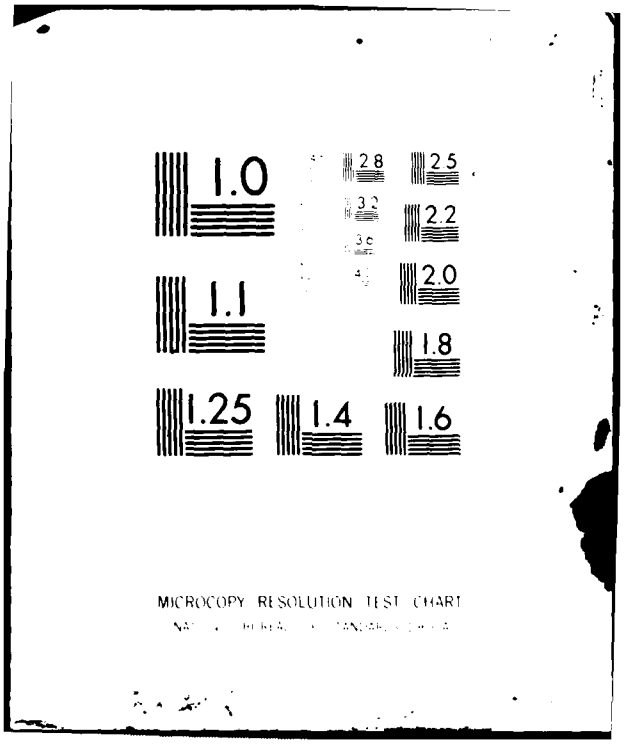
1.0
2.8
2.5
3.2
2.2
3.6
4.0
2.0
1.1
1.8
1.25
1.4
1.6
MICROCOPY RESOLUTION TEST CHART

(12)

A Final Technical Report
Prepared Under Grant No. N00014-75-C-0691

STRUCTURAL CHARACTERIZATION OF SCHLADITZ WHISKERS

Submitted to:

Office of Naval Research
Department of the Navy
800 North Quincy Street
Arlington, Virginia 22217

Attention: Metallurgy Division
Code 471

Submitted by:

H. G. F. Wilsdorf
Professor

Report No. UVA/525321/MS82/104
May 1982

SCHOOL OF ENGINEERING AND
APPLIED SCIENCE

DEPARTMENT OF MATERIALS SCIENCE

UNIVERSITY OF VIRGINIA
CHARLOTTESVILLE, VIRGINIA 22901

A Final Technical Report
Prepared Under Grant No. N00014-75-C-0691

STRUCTURAL CHARACTERIZATION OF SCHLADITZ WHISKERS

Submitted to:

Office of Naval Research
Department of the Navy
800 North Quincy Street
Arlington, Virginia 22217

Attention: Metallurgy Division
Code 471

Submitted by:

H. G. F. Wilsdorf
Professor

Department of Materials Science
RESEARCH LABORATORIES FOR THE ENGINEERING SCIENCES
SCHOOL OF ENGINEERING AND APPLIED SCIENCE
UNIVERSITY OF VIRGINIA
CHARLOTTESVILLE, VIRGINIA

Report No. UVA/525321/MS82/104
May 1982

Copy No. 19

SECURITY CLASSIFICATION OF THIS PAGE (When Data Entered)

REPORT DOCUMENTATION PAGE		READ INSTRUCTIONS BEFORE COMPLETING FORM
1. REPORT NUMBER	2. GOVT ACCESSION NO. AD-A115 098	3. RECIPIENT'S CATALOG NUMBER
4. TITLE (and Subtitle) Structural Characterization of Schladitz Whiskers		5. TYPE OF REPORT & PERIOD COVERED Final Report 02/01/76 - 02/28/82
		6. PERFORMING ORG. REPORT NUMBER UVA/525321/MS82/104
7. AUTHOR(s) H. G. F. Wilsdorf		8. CONTRACT OR GRANT NUMBER(s) N00014-75-C-0691
9. PERFORMING ORGANIZATION NAME AND ADDRESS University of Virginia School of Engineering and Applied Science Charlottesville, VA 22901		10. PROGRAM ELEMENT, PROJECT, TASK AREA & WORK UNIT NUMBERS
11. CONTROLLING OFFICE NAME AND ADDRESS Office of Naval Research Department of the Navy Arlington, VA 22217		12. REPORT DATE May 1982
		13. NUMBER OF PAGES
14. MONITORING AGENCY NAME & ADDRESS(if different from Controlling Office)		15. SECURITY CLASS. (of this report) Unclassified
		15a. DECLASSIFICATION/DOWNGRADING SCHEDULE N/A

16. DISTRIBUTION STATEMENT (of this Report)

Distribution Unlimited

This document has been approved for public release and sale; its distribution is unlimited.

17. DISTRIBUTION STATEMENT (of the abstract entered in Block 20, if different from Report)

N/A

18. SUPPLEMENTARY NOTES

N/A

19. KEY WORDS (Continue on reverse side if necessary and identify by block number)

steel
microdispersion
bond strength
filaments
alloy strengthening

20. ABSTRACT (Continue on reverse side if necessary and identify by block number)

Polycrystalline iron whiskers containing 1.5 w/o C and 0.8% O have an extraordinary ultimate tensile strength between 6 and 8 GPa. Their microstructure has been investigated by transmission electron microscopy and electron diffraction techniques. It has been found that the whiskers consist of α-Fe grains between 2 nm and 30 nm in diameter which do not have sharp boundaries but are separated by a wide boundary region. A microdispersion of α-Fe, Fe_3O_4, Fe_3C, α-Fe_2O_3 and carbon is prevalent throughout the

DD FORM 1 JAN 73 1473 EDITION OF 1 NOV 65 IS OBSOLETE

Unclassified

SECURITY CLASSIFICATION OF THIS PAGE (When Data Entered)

whisker volume. Again, no sharp phase boundaries seem to exist which could imply a transitional region between second phase particles characterized by a concentration gradient and mixed covalent and metal bonding. It is concluded that a new strengthening mechanism for alloys is responsible for the mechanical properties of CVD produced steel whiskers. This mechanism requires a grain size below 30 nm, non-planar grain boundaries and a microdispersion of particles of iron oxides, iron carbides and carbon. Also, the covalent/metallic bonding mix within the transition region between the minute second phase particles and the α-Fe matrix is considered an essential component of the strengthening mechanism.

SECTION I

INTRODUCTION AND SCIENTIFIC BACKGROUND

The considerable effort that has been expended on whisker research in the fifties and early sixties was initiated by the discovery of the great specific strength of metal whiskers, by Herring and Galt[1] for the case of tin whiskers, that prompted the expectation that by the use of whiskers, superstrong materials could be produced.

Best known with respect to the extraordinary strength of whiskers is the work by Brenner[2,3] who was the first to show that whisker strength decreases with increasing diameter, d, finding for iron whiskers the relationship[2]

$$\sigma_{Av} = \frac{1630}{d} - 50 \ (kg/mm^2), \text{ if d is measured in microns,}$$

where σ_{Av} is the average ultimate tensile stress of whiskers of same diameter, d. This remarkable dependence of strength on whisker diameter was subsequently confirmed[3-6] and is currently accepted in the literature as a rather fundamental property of whiskers.

The highest strength found by Brenner for any iron whisker was a little less than 1350 kg/mm^2, the next highest about 550 kg/mm^2, at diameters of about 1.5 and 3.3 microns, respectively,[2] and the former value has remained to be the highest ever reported. All iron whiskers examined by Brenner were single crystalline, and all fractured without warning and without detectable preceding plastic deformation.[2]

Throughout the period during which there had been an intensive research interest in whiskers within the international scientific community, say, between 1952 and 1970, and up to the present time, it has been taken as axiomatic that strong metal whiskers are nearly perfect single crystals. The

similarly wide-spread notion that whiskers were discovered only recently, lacks any factual basis. Thus, in their survey article on the growth of crystal whiskers, Nabarro and Jackson[7] adduce numerous references describing observations on whiskers of many different kinds, extending back as far as 1574.[8] Among the 250 references pertaining to whiskers,[7] Nabarro and Jackson have included forty-seven dating from 1930 and earlier, with quite a few of these written before this century.

The "Schladitz-Whiskers" are grown from the gaseous phase by the chemical decomposition of some suitable carbonyl or other metal-containing gas on substrates at elevated temperatures. A schematic diagram of the apparatus invented by H. J. Schladitz for this purpose has been given by Dawihl and Eicke[9] and a photograph of it is given in Figure 1. The decisive principle involved, besides the well-known thermal decomposition of metal carbonyls, is the use of a magnetic field to keep the whiskers straight while they are still extremely thin. It appears that the whiskers are formed in their full length of typically one or a few mm almost instantaneously, and then thicken by the further deposition of metal.[10] Schladitz[10,11,12,13] as well as Dawihl and Eicke[9,14] have investigated the most important physical properties of these whiskers, focusing their attention primarily on iron whiskers. Their properties include the following: the grain size in the as-deposited state is about 90 Å. Recrystallization in iron whiskers begins at about 300°C.[11] As indicated in Figure 2, the tensile strength of the whiskers is largely independent of diameter,[12]--in stark contrast to the discussed behavior of single crystalline metal whiskers--and lies between 500 and 800 kp/mm^2 for carefully produced whiskers with diameters between about 0.1 and 50 microns.[10] In 'pure' whiskers the strength drops to about 200 kg/mm^2 at 600°C, but for whiskers containing 2.5% Cr, the micro hardness and, hence, by inference

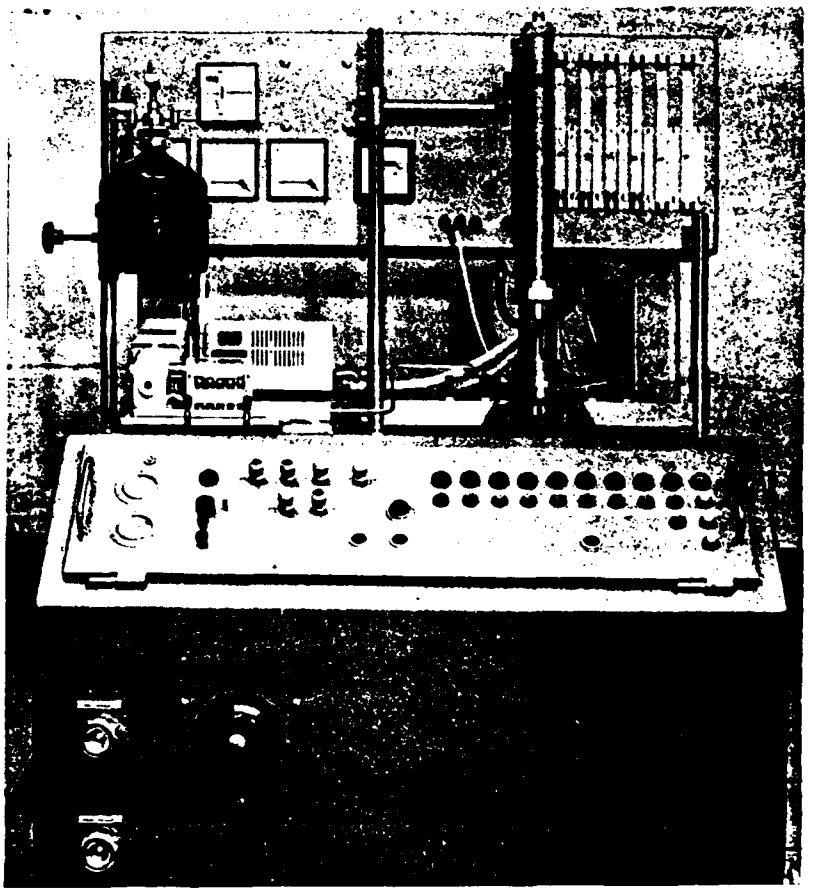

Figure 1. Schladitz whisker machine. For additional information see H. J. Schladitz, German Patent No. 1224934 (1964), U. S. Patents No. 3441408 and No. 3570829 (1969/1971).

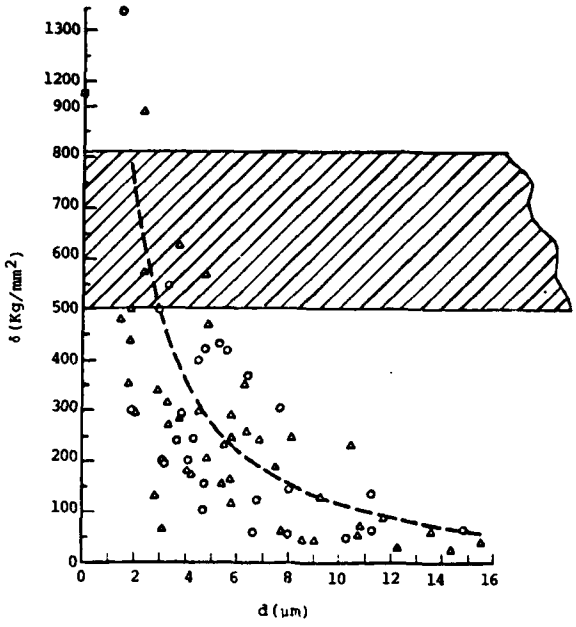

Figure 2. Published values for the tensile strengths of single crystal iron whiskers (apparently extracted from refs. 2 to 6), revealing the considerable scatter in experimental values and the dependence of whisker strength on diameter, as compared to the strength of polycrystalline iron Schladitz whiskers (shaded region) as given in ref. 12, based on W. H. Sutton and H. W. Rauch, Sr. (*General Electric Information* Series, R66SD46, Aug. 1966).

the tensile strength, remains constant up to 800°C, and at 1000°C is only 20% lower than at room temperature.[9,11,14]

The microstructure of 'pure' iron whiskers reveals two intermingled phases of unknown chemical composition, or a third phase by itself.[9] Certainly, the material is not in thermodynamical equilibrium as judged from the Fe-C-O constitution diagram.[9,14] In the as-grown state, the so-called 'pure' iron whiskers, i.e. those which have not been deliberately alloyed, contain in excess of 1% carbon, about 80% of which is in free form, a similar amount of oxygen, and in the order of 0.04% nitrogen, and thus are in composition the same as carbonyl iron powder.[9] The coercive force of Schladitz-whiskers of iron is roughly 50% of that of carbon steels.[9,14]

For the practical applicability of Schladitz-whiskers it is of extreme importance that they are of nearly uniform thickness within any one batch made and also have similar lengths and tensile strengths as well as microhardness.[12] On a very fine scale, however, the whisker surfaces are not smooth but are covered with rounded protuberances. This is a welcome feature since it facilitates the bonding between whiskers and matrix when composites are made. Moreover, the surface roughness, and thus the surface to volume ratio, can be deliberately influenced.[10] According to a diagram published by Schladitz,[13] the surface area, A, measured in square meters (m^2), per gramme of iron is related to the average whisker diameter, d, as $A \cong 13\ (m^2)/d$ if d is measured in microns and the whiskers are made deliberately rough surfaced, while the normally 'smooth' whiskers yield $A \cong 4\ (m^2)/d$. By contrast, Dawihl and Eicke[9] quote a specific surface value of 0.3 m^2/g for carbonyl iron powder. Thus, since whiskers with diameters of 1 micron and less can be readily made, the surface to volume ratio of Schladitz whiskers can be made quite large.

As the whiskers grow by thermal decomposition of carbonyls out of the gas phase, they may be deliberately alloyed by the simultaneous deposition of two or more substances, including nickel, chromium, tungsten, oxides and carbides, or, alternatively shells of different chemical composition may be laid down one on the other.[12] Hence, also, iron whiskers may be nickel- or chrome-plated to impart to them corrosion resistance if their intended use should demand this.

It was the objective of this research to relate the microstructural features of CVD steel filaments to their extraordinary strength in tensile loading. X-ray and electron diffraction, transmission electron microscopy (including analytical techniques), field ion microscopy and Mössbauer studies were employed in this research.

SECTION II

RESULTS

A. Analytical Whisker Apparatus

With an increasing understanding of the growth of steel whiskers and their properties, certain refinements in production techniques and investigational methods were required.

Some changes have been made which have rendered the Schladitz whisker machine more versatile: (a) the magnetic field strength was increased from 0.125 T to 0.22 T; and (b) "analytical" screens as anchoring substrates were used throughout; (c) a new set of flowmeters was installed allowing a precise control of gas flow; (d) the pulsating finger pump was replaced by a glass reservoir with precision metering valve. Adjusting the nitrogen pressure, carbonyl flow rates can be controlled for continuous introduction into the vaporizer.

The last two changes reduce the probability that gas and carbonyl flow instabilities are produced in the reaction space, and the screen arrangement permits the removal of the whiskers without damage and preserves the space location where they were grown. A thermocouple system was completed and tested on the whisker apparatus. The thermocouple inputs could be recorded simultaneously on a point recorder or could be seen at will on a digital read-out meter without affecting the recordings. A feedback capability could anticipate trends of temperature changes and thus permit the maintenance of predetermined temperatures.

The following temperature measurements were obtained for the Schladitz apparatus. Temperature control in this machine is by thermostatic control which allows predetermined temperature schedules. Temperature measurements have been made for thermostat readings between 390°C and 250°C which

correspond to actual temperatures in the reaction cylinder between 320° and 180°C. Also temperature gradients were determined at three levels in the cylinder. Near the top of the reaction zone the temperature drop from the hot region to the low temperature region (i.e. to the center carbonyl vaporizer) is 20°C for the thermostat setting of 320°C which corresponds to an actual decomposition temperature of 245° to 265°C. In the central and lower zone of the reaction cylinder the temperature gradient is 5°C only.

B. General Microstructure

The Schladitz process involves the decomposition of iron pentacarbonyl in the presence of a magnetic field which has to be homogeneous throughout the reaction space. The whiskers described in the following pages were mostly grown at a field strength of 0.125T. Fe $(CO)_5$ decomposes over a temperature range of about 150°C to 280°C; the temperature dependent deposition rate is known.[15] One can safely assume that the first iron crystals are produced by gas phase nucleation at about 260°C. They arrange themselves into stringlike assemblies parallel to the magnetic field lines and thus form the "core" of the whiskers. Then, the temperature is generally adjusted to a lower level where gas phase diffusion is the predominant mechanism of deposition and the whiskers are grown to the desired thickness over a period from 3 to 20 minutes or even longer. In addition to temperature, carbonyl flow rate and magnetic field strength, reaction space geometry, nucleation surfaces, types and pressure of carrier gases, and exhaust conditions are the most important variables; they also will affect the chemical composition of the whiskers. They normally contain between 1 and 1.8 w/o of carbon and 2.8 w/o oxygen plus 0.01 w/o nitrogen and possibly insignificant amounts of metallic impurities. A careful chemical analysis of the whiskers was made by Dawihl and Eicke,[9,14] Lashmore,[16] and Newkirk and Wilsdorf.[17]

The ultimate tensile strength (UTS) of polycrystalline steel whiskers has been reported to reach almost 8 GPa (800 Kg/mm^2).[11,14] In contrast to single crystal whiskers the polycrystalline whiskers UTS is not dependent on whisker diameter. Tensile testing of the whiskers is delicate and time consuming and most data are reported for the convenient thickness range of 5 to 30 μm. Frequently, microhardness tests are employed for strength determinations since a conversion from pyramid hardness to ultimate strength can be made[18,19]; a confirmation of this relationship for the steel whiskers has been obtained.[16] Measurements of UTS by three independent researchers at the University of Virginia yielded average values of 3.8 GPa, 3.6 GPa and 3 GPa for the best batches with maximum values of 6 GPa, 4.2 GPa, and 5 GPa, respectively.[16,20,21] Whiskers can be obtained with diameters in excess of 100μm but tensile tests have not been conducted on whiskers thicker than 30μm. Larger diameter whiskers often can be observed to have surface cracks in an approximately axial direction, and it is anticipated that they may have reduced strength. In regard to mechanical properties we will limit our discussion to whiskers in the 5μm to 30μm range. The whiskers fail in a brittle fracture mode.

Polycrystalline steel whiskers have an extremely small grain size which ranges consistently between 5 nm and 30 nm, occasionally becoming as large as 50 nm. Figure 3 shows the typical microstructure of the whiskers as seen by transmission electron microscopy (TEM). Many grains are not transparent which does not indicate that they are thicker but rather that double diffraction diverts the primary electrons on account of two or more crystallites lying on top of each other in the direction of the electron beam. The grains do not contain dislocations unless they are present in grain boundaries. Even when the electron beam transmits a single grain which is not in diffraction

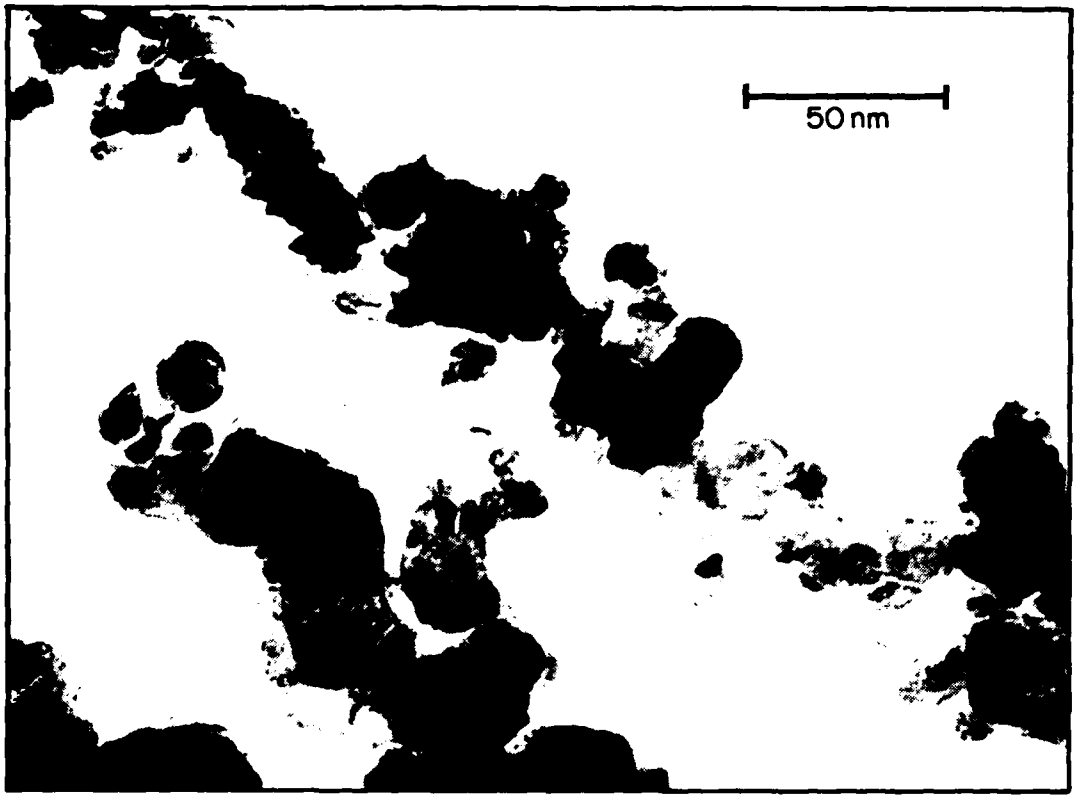

Figure 3. Transmission electron micrograph showing the very small grain size of steel whiskers between 5 nm and 30 nm. Note mottled background in transparent grains.

orientation, the crystallites appear with a mottled background. Details of this unusual phenomenon have been clarified recently by a field ion microscope study (FIM) by Inal and Murr[22] who found that the crystallites did not have a "long-range" crystallinity but were frequently disturbed by many regions different from the iron lattice. Figures 4a and 4b illustrate several typical field-ion images. These field-ion micrographs are lacking in the surface atomic symmetry and detail normally associated with field-ion images of metal and alloy emission end forms, but they are typical of the images which could be obtained using helium image-gas imaging at 78 K. The images of Figure 4 show several features of the whisker microstructure. First, it should be

apparent that there is no "long-range" crystallinity. Figure 4a shows that grain sizes characteristic of individual crystallites are generally about 2nm. Furthermore, the images in Figure 4 contain numerous, large image points which can be interpreted as being carbon or carbonlike,[23] or molecular in nature, i.e. they could be carbides or oxides. Previous X-ray studies have indicated that carbon, carbides, and oxides are incorporated into the whisker microstructure.[9] Figure 4 shows that such inclusions are distributed somewhat randomly within the microstructure, and not restricted to the grain boundaries.

The fact that the field-ion images are somewhat restricted to short-range order or small crystallite areas is due in part to the fact that the minimum tip radius will be determined to a large extent by the sizes of the crystallites composing the core or center of the individual fibers. In Figures 4a and b, however, only the central core structure forms the image. This is because the electroetching produces a systematic removal of the outer surface shells as the end form or tip is created at the core. Consequently, the images of Figures 4a and b confirm that some of the grains at the actual core are roughly 2 nm. The grain size of α-iron in the core and in the concentric cylindrical shells surrounding the core, varies between 2 and 30 nm depending on the local conditions governing the CVD process. Figures 4a and b are illustrating this difference in the grain size. No grain boundaries were apparent, and there was, as noted above, little crystal order in excess of regions measuring 2 to 5 nm in size. A great deal of the image points were unstable and images of single points (atoms or molecules) would appear, split into two arcs, grow, and disappear as if some gas or other species was being drawn from the specimen by the high field condition.

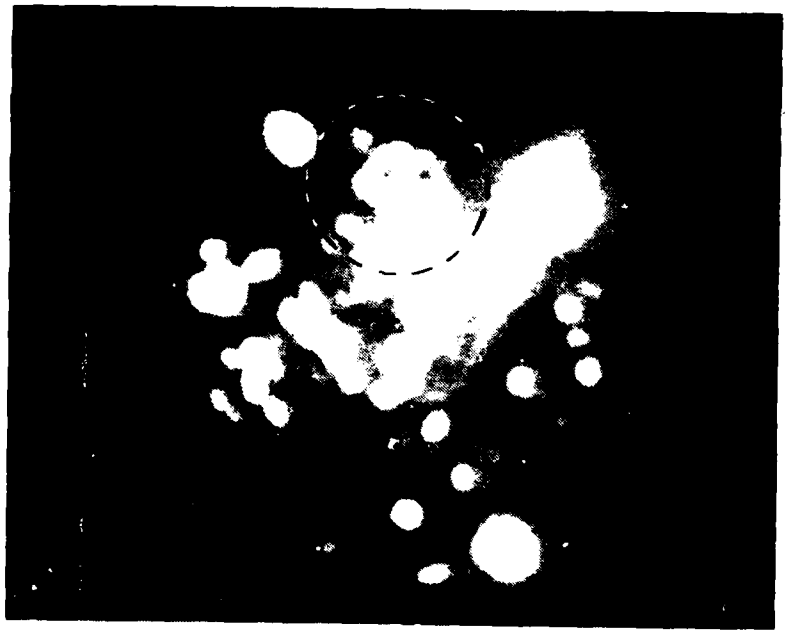

Figure 4a. Field ion microscope images of Fe-C filaments. Edge-plane structure characteristic of small crystallite of α-Fe is shown circled. Crystal (grain) sizes measured from these observations averaged roughly 2 nm.

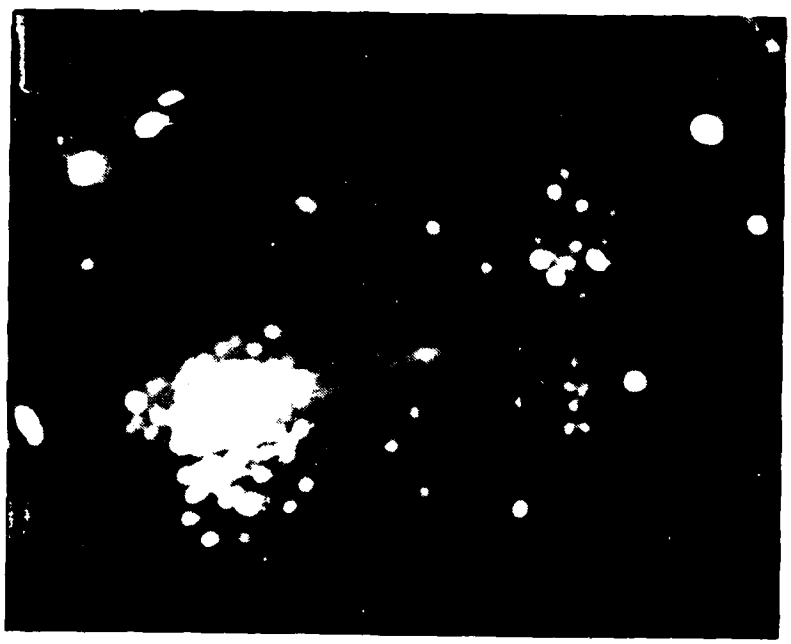

Figure 4b. Large image spots and streaks suggestive of inclusions of carbon, carbides or oxides within the microstructure. The structure is characteristically "amorphous."

X-ray and electron diffraction patterns were obtained in order to determine in which form carbon and oxygen were present in the whiskers. Table I lists measurements of d-values from X-ray and electron diffraction patterns together with estimated intensities. Also, the d-values for α-Fe, α-Fe_2O_3, Fe_3O_4, Fe_3C, and graphite have been listed and it is seen that a number of these substances frequently have d-spacings which coincide. X-ray and electron diffraction lines 9, 18, 20, 21 are unambiguously due to α-Fe. The presence of Fe_3O_4 and Fe_3C is clearly indicated in the X-ray diffraction data and, taking into account the overlap, the agreement with expected intensities is fair. Traces of α-Fe_2O_3 seem to be present, but graphite is not indicated.

Electron diffraction patterns hold some special interest for the analysis in that four lines are made up primarily from spots while the remaining five lines have a uniform intensity. All spotty lines are associated with α-Fe rings while lines 1, 2, 4, 15 and 17 have the d-spacings of Fe_3O_4. Although lines 4 and 15 coincide with d-spacings of Fe_3C, the intensities of the former are (100) and (85) compared to the intensities of Fe_3C (5) and (7). Also, the strongest Fe_3C line, No. 3, is absent in the electron diffraction pattern. The spottyness of the iron rings was to be expected from the electron micrographs and agrees well with the grain size measurements of up to 30 nm. The rings ascribed to Fe_3O_4 with their homogeneous intensity, on the other hand, must be caused by crystals less than 5 nm size.

C. Effect of Magnetic Field on Strength

The role played by the magnetic field on the production of whiskers obviously is a very important aspect of understanding the strengthening mechanism. Ejim[20] investigated seven batches of whiskers produced at 0.016, 0.03, 0.072, 0.09, 0.126, 0.18 and 0.22T. His results are shown in Figure 5. The strength of the whiskers increased with magnetic field strength up to

TABLE I

X-Ray and Electron Diffraction Data from Whiskers

Ref. No.	X-Ray Diffr.	d-values α-Fe	Fe_3O_4	Fe_3C	α-Fe_2O_3	Graphite	Electron Diffraction
1	2	3	4	5	6	7	8
1			0.485 (40)		0.366 (25)	0.336 (100)	0.481 w cont.
2	0.298 (4)		0.297 (70)				0.299 w cont.
3	0.268 (6)				0.269 (100)		
4	0.254 (21)		0.253 (100)	0.254 (5)			0.256 m cont.
			0.242 (10)				
				0.251 (50)			
5	0.240 (12)		0.238 (65)	0.238 (65)			
6	0.228 (10)			0.226 (25)			
7	0.223 (10)			0.220 (25)			
						0.213 (10)	
8	0.210 (14)		0.209 (70)	0.210 (60)			
				0.206 (70)			
9	0.203 (st)	0.203 (100)		0.202 (60)	0.202 (30)	0.203 (50)	0.203 st spotty
				0.201 (100)			
10	0.194 (9)			0.197 (55)			
11	0.188 (12)			0.187 (30)			
12	0.186 (16)			0.185 (40)		0.180 (5)	
13	0.176 (6)			0.175 (15)			
14	0.169 (5)		0.171 (60)	0.169 (15)	0.170 (60)	0.168 (80)	
15	0.162 (7)		0.161 (85)	0.161 (7)			0.162 w cont.
16	0.159 (8)			0.158 (20)		0.154 (10)	
17	0.149 (10)		0.148 (85)		0.148 (35)		0.149 m cont.
					0.145 (45)		
18	0.143 (100)	0.143 (19)					0.143 m spotty
19	0.132 (5)		0.132 (20)				
						0.123 (30)	
20	0.117 (st)	0.117 (30)				0.116 (50)	0.116 st spotty
						0.114 (5)	
						0.112 (20)	
21	0.101 (32)	0.1013 (9)					0.104 w spotty

( ) estimated intensities, w = weak int., m = medium int., st = strong int.,

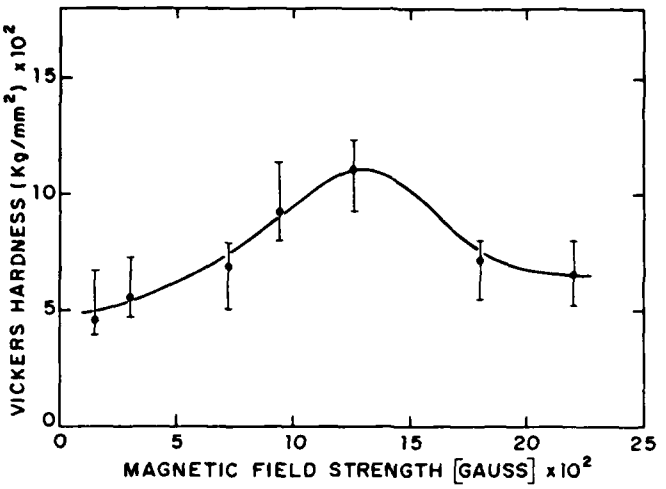

Figure 5. Dependence of microhardness of magnetic field strength for Fe-C Whiskers.

0.125T and then declined again. The effect has not been explained as yet, despite efforts to discern differences in microstructure by TEM. Grain sizes and other microstructural details are all comparable for the seven runs made.

After having found that the maximum strength occurred when applying a field of 0.125T, whiskers were characterized also as to their diameter, length, and surface topography. Eight runs were monitored from zero to 0.22T and the range of diameters is listed in Table II below. Only at low magnetic fields is the effect significant. Viewing whiskers at low magnifications in the electron microscope one finds that "macroscopically" the whisker alignment parallel to the field is poor for the runs at low field strengths.

Further, it was found that the strength was not dependent on diameter for whiskers > 10 μm as determined by microhardness tests. Since in the course of this specific investigation whiskers were grown routinely to diameters > 20 μm, it was observed by scanning electron microscopy that many whiskers had developed cracks at their surfaces after exceeding a thickness

TABLE II

Typical Maximum Range of Diameters for Whiskers Produced at Different Field Strengths

Magnetic Field Strength (Tesla)	Range of Diameters (μm)
0	no whiskers
0.016	7 - 10
0.030	10 - 15
0.072	15 - 20
0.090	22 - 40
0.126	30 - 57
0.180	30 - 50
0.220	30 - 52

of 30 μm. The length of the whiskers varies for these runs between 0.25 mm and 5 mm independent of field strength applied.

The surface topography of whiskers depends on their thickness regardless of field strength. Up to diameters of 15 μm the surface exhibits nodular features while whiskers thicker than 15 μm have ring-like ridges. All whiskers have a well-rounded end geometry.

D. Mössbauer Study

Despite some concentrated efforts the position of carbon atoms remained obscure. Earlier it had been speculated by Lashmore that carbon might have combined with Fe to form Fe_3C. No iron carbide was detected by X-ray or electron diffraction methods in the virgin whiskers. In order to check the possibility of a size effect, a Mössbauer investigation was conducted.

Mössbauer measurements were made for two samples. Sample 1 was prepared by grinding whiskers to powder and mixing them with boron nitride to produce a sample thickness of 20 mg/cm^2. Sample 2 was prepared by placing whole whiskers in a sample holder in such a way that all the whiskers lie perpendicular to the incident gamma rays.

An Austin Science Assoicates model S-3 constant acceleration spectrometer was used together with an Amperex xenon methane proportional counter, and a Nuclear Data model 2200 multichannel analyzer. The source material used for sample 1 is ^{57}Co in Cu. The source for sample 2 is Co ^{57}Cr, kindly loaned to us by the Spire Corporation of Bedford, Massachusetts. Both experiments were performed with transmission geometry and with source and absorber at room temperature. The data was fit to a six line Lorentzian curve using an iterative least squares fitting program on an IBM 370/165 computer. The spectra were fit to a six line magnetically split pattern with no quadruple splitting. The widths of all six lines were constrained to be the same and the intensities of the lines were pair-wise constrained to be equal. The spectrometer was calibrated using an α-Fe foil. Velocities shown in the figure are relative to α-Fe.

The spectrum of sample 1 (Fig. 6) is basically that of α-Fe. However, the peaks are broadened on the inner side and the regions between the peaks

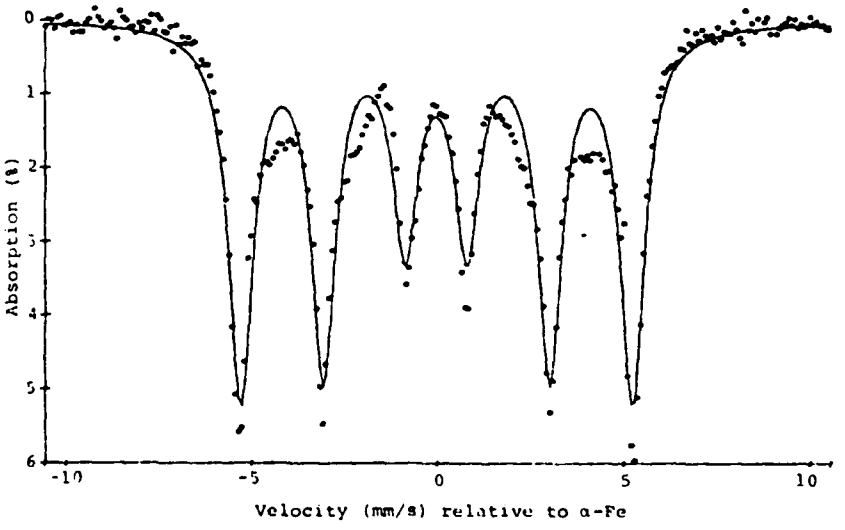

Figure 6. Mössbauer spectrum of powdered polycrystalline iron whiskers. The solid line represents the constrained least squares fit described in ref. 24.

show the presence of other species. The widths of the six major peaks are essentially the same. The spectrum of sample 2 differs from that of sample 1 only in the line widths. This difference is due to the greater line width of the Cr source.

Perhaps the most startling conclusion to be drawn from these spectra is that essentially none of the carbon in the whiskers is in the form of Fe_3C. Other carbides are likely present, however, and probably account for the small peaks in the region between the major peaks. The broadening of the major peaks is most likely caused by superparamagnetism. This indicates that the very small grain size observed in the tiny precursors of whiskers is found throughout larger whiskers as well. The broadening is probably not caused by a distribution of magnetic fields because the six lines have equal widths. The similarity of the spectra in Figure 6 indicates that the direction of magnetization of the magnetic domains in this material is essentially random.[24]

The whiskers used in this study were produced by the decomposition of Fe $(CO)_5$ in a magnetic field of 0.13T. Whisker growth was initiated at 265°C and within 3 minutes reduced to 200°C; the run was completed after 31 minutes at 200°C. N_2 and $C0_2$ were used as carrier gases.

A similar Mössbauer study was conducted at the National Bureau of Standards.* Also, a whisker sample produced at the University of Virginia was being used, although it was made in the original Schladitz machine. The difference between the two specimens can be traced to using different carrier gases and different decomposition temperatures. The results obtained by the NBS were different from our own study in that carbon was found to have

* Private communication by D. S. Lashmore, L. J. Swartzendruber and L. H. Bennett.

combined with Fe to Fe_3C. It was calculated that 18 $\pm$ 2% of carbon atoms were tied up in iron carbide.

We have checked the results obtained at the NBS and an opportunity was given the NBS group to review our investigation. There is mutual agreement that the samples tested were different. Electron diffraction patterns taken from these specimens recently also showed differences. It is now clear that the composition and distribution of microprecipitates in the whiskers depends on both decomposition temperature as well as on the specific carrier gases used.

E. Microstructural Changes at Elevated Temperature

The unique microstructure of the CVD steel whiskers is due to its "assembly" between 280°C and 200°C which is nearly an order of magnitude lower than going from the melt through a solidification process. Annealing experiments were designed to study changes in the microstructure. The questions that were to be answered first relate to the growth of α-Fe crystallites as well as to the rearrangements in microdispersion with a possible phase change. Schladitz[11] and Dawihl and Eicke[9] had reported a reduction of hardness after annealing at 300°C which was found to lower the original value of 1,450 Kg/mm^2 to 550 Kg/mm^2 after annealing for 15 minutes at 500°C. Also, our X-ray diffraction results indicated that a heat treatment at 500°C produced either an increase of the amount of Fe_3C or the agglomeration of small clusters to larger crystals.

It was thought that in-situ annealing experiments in the Philips EM 400 would be the best approach to obtain the required information. Firstly, the high resolution of the instrument would permit a recording of the microstructural changes in great detail and secondly, chemical changes could be followed by electron diffraction. A series of experiments was conducted raising the

temperature slowly up to and beyond the transformation point, obtaining the FCC structure of iron which was recorded at the completion of the run.[25] Noticeable changes in the grain size took place at temperatures above 500°C. For example, raising the temperature to 550°C for 10 to 15 minutes resulted in a grain size of the α-Fe crystallites to about double the size of the original structure. Further, another significant observation could be made: the mottled contrast in electron transparable grains which is characteristic for the original steel whiskers, had almost disappeared. Electron diffraction patterns were taken with each group of micrographs, so that microstructural changes could be correlated with chemical changes. Some details of the TEM study follow.

Since the typical temperature range for whisker production is between 160°C and 270°C, it must be expected that some or all of the foreign inclusions are metastable. If indeed this would be so, changes in the electron diffraction patterns could be expected at temperatures above the growth temperature of the whiskers. In-situ annealing experiments up to 920°C were conducted. The first noticeable change in the whisker grain size took place at about 550°C. Diffraction patterns taken at 550°C and 569°C contain diffraction rings of both α-Fe and Fe_3O_4 and the rings of α-Fe, respectively. The most obvious difference in the α-Fe rings visible in the diffraction patterns at 550°C and 569°C is the number and size of the spots which make up the rings. Larger but fewer spots at 569°C indicate that grain growth took place between 550°C and 569°C. Remarkable is the absence of Fe_3O_4 rings at the higher temperature. Annealing above the transformation temperature at 920°C produced the diffraction pattern of γ-Fe.

A sequence of four TEM micrographs taken during an in-situ anneal permits to follow the grain growth between 550°C and 920°C. At room tem-

perature whiskers have a grain size between 5 nm and 30 nm with an average grain size between 10 nm and 20nm; contrast for individual grains is not uniform but many dark or light dots, depending on background, about 2 nm in diameter are discernable. Grain boundaries are poorly defined. Bringing the specimen to 550°C in 15 minutes and holding in at that temperature for 10 minutes indicates grain sizes between 10 nm and 70 nm with an average size of about 30 nm. Grain boundaries have become distinctly sharper. Thickness fringes are visible which are evidence for flat grain boundaries. Also, the mottled appearance of electron transparent grains has almost vanished. At 704°C little change in grain size occurred but grain boundaries have continued to sharpen and are now well defined. All grains are now electron transparent. The final micrograph was taken after an anneal of 920°C and cooling the specimen to room temperature within 4 minutes. Grains have grown to diameters of 0.1 μm or larger, and their boundaries are sharp; however, precipitates are visible at or near the grain boundaries in some of the grains.

A careful examination of grain boundaries in high resolution TEM micrographs (~1 nm) reveals that the boundaries lack the usual definition. Although the grain boundaries must provide for orientation changes, they are not abrupt but can best be described as transitional regions having a width not less than the particles in the microdispersion and often appear to be wider. This concept excludes by its very nature the development of sharp grain boundary ledges. Often, grains do not meet at sharp nodal points but have rounded corners. At triple nodes one can observe occasionally through subtle contrast changes that additional material had been added where the three grains meet. No micro-porosity has ever been detected. This is understandable since the decomposition of $Fe(CO)_5$ under our growth conditions

takes place largely on the whisker surfaces leading to continuous surface diffusion during the growth process. Grain boundaries are often becoming visible in TEM investigations through fringe contrast (Murr[26]). However, this characteristic contrast was not seen in whiskers which is further evidence for poorly defined grain boundaries and for grains with non-planar boundaries. Only after annealing to 570°C and 704°C was fringe contrast observed, indicating the development of grains with planar boundaries.

F. Microstructural Observations Made on Thick Filaments

The TEM results obtained so far were from the transmission of electron transparent filaments, sticking out from thicker filaments. A new preparation technique was applied, to thin down thick filaments (20 μm) by ion sputtering. The data obtained in this fashion confirmed the general results described above but also permitted a number of new conclusions based on analytical high resolution TEM results.[27]

The grain size of α-Fe inside the filaments comprises the same range as before, namely 30 nm to 5 nm; however, the range to lower values had to be extended to 3 and 2 nm. This is a most interesting result in that it brings down the α-Fe grain size into the range of particles representing the microdispersion. SAD patterns confirmed the size of Fe_3O_4 particles to be about 3-2 nm in agreement with earlier measurements. Center beam dark field techniques revealed a new distribution of iron grains. Often, they formed clusters with the grains having a similar crystallographic orientation. Again, grain boundaries were found to have a finite width between 1 and 2 nm. In general, it can be concluded that the microstructure is similar throughout the filaments as reported earlier, although special structures such as clustering came to light.

G. Alloying of Cr to Fe Filaments

Attempts were made to alloy Cr to Fe by CVD techniques.[21] A study which successfully achieved such an alloying through the work of Moore yielded a number of interesting results and may serve as an indication that unexpected difficulties in the alloying process may be encountered.

As has been reported in the literature, steel whiskers produced according to the Schladitz CVD process are losing their strength in the temperature range between 400°C and 1,000°C, while chromium-steel whiskers would retain their strength to 23% of their initial strength at 1,000°C but the loss at 800°C would virtually be negligible.[28] This part of the study had as its objective (1) a confirmation of the above result; and (2) to provide an explanation for the strengthening in chromium alloyed steel whiskers at elevated temperatures.

The apparatus for the production of chromium containing iron whiskers is shown in Figure 7. Eight batches of chromium-iron whiskers were produced and analyzed. The research involved five major efforts:

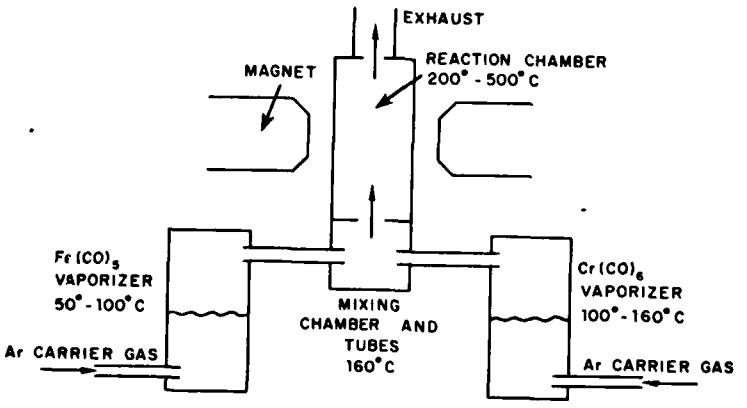

Figure 7. Diagram of filament producing apparatus using independent vaporization of carbonyls.

(1) a determination of the chromium content in the whiskers

(2) the determination of the whisker strength

(3) the determination of the strength after annealing at 400, 600 and 800°C

(4) the determination of the microstructure

(5) the correlation between microstructure and strength

The experimental technique for the production of chromium containing whiskers has been described in detail in the dissertation by Thomas Moore.[29] On account of the difference in vapor pressures for the carbonyls of iron and chromium the whisker production in each batch was not uniform in respect to chromium content. The distribution of chromium in individual whiskers showed a very high chromium content in whiskers near the input end of the whisker collection screen and a much lower and more slowly decreasing chromium content in whiskers further from the input end. However, this result was reproducible and a typical distribution curve of chromium in individual whiskers in shown in Figure 8. This distribution implies a very rapid preferential deposition of chromium and a subsequent depletion of chromium carbonyl from the reactant vapor. The chromium containing whiskers were being grown by first producing a very thin pure iron core and then permitting the mix of iron and chromium carbonyls to produce the final whisker. As can be seen in Figure 9, the diameter of the whiskers also changed from a large diameter (approximately .9 mm) at the input edge to whiskers in the low micrometer range at the output edge. The average length of whiskers was on the order of 4 mm.

A quantitative X-ray analysis was carried out by an energy dispersive X-ray analyzer connected to a scanning electron microscope. Two major results have been obtained. Firstly, as the chromium content of the whiskers

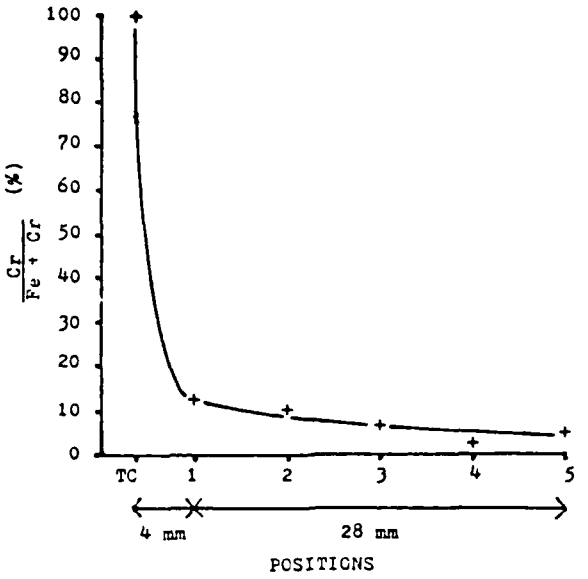

Figure 8. Distribution of chromium in individual whiskers for Experiment #5 expressed by the intensity ratio, in percent, of Cr K radiation intensity over the sum of the Fe and Cr K radiation intensities. Position TC signifies a point on the reaction chamber thermocouple shaft about 4mm before the input edge of the collection screen. Position 1 denotes the input edge of the collection screen and subsequent positions were spaced at 7 mm intervals along the central axis of the reaction chamber with position 5 denoting the output edge of the collection screen.

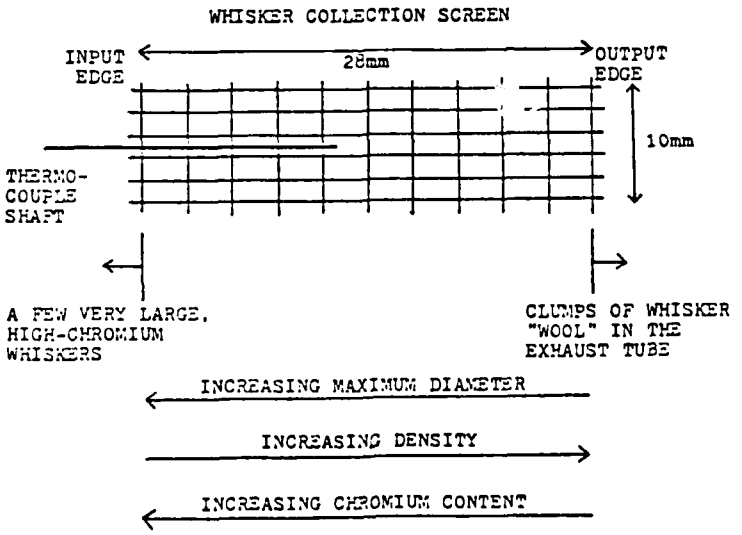

Figure 9. Description of the major characteristics of alloy whisker growth on the collection screens used in this study.

was increased, the fraction of the total mass of the sample volume that was being detected decreased continuously to approximately 75% in the chromium whiskers. Secondly, this decrease in the fraction detected was independent of the heat treatment. Due to absorption of lower energy X-rays by the beryllium window of the detector the technique is insensitive to elements of atomic number less than 11. From a consideration of the elements present during whisker growth and from the X-ray diffraction analysis, the elements that would be expected to make up the difference in mass are carbon and oxygen. Assuming that the carbon content in chromium containing steel whiskers is the same as in pure steel whiskers, namely 1.5 weight percent, one would expect that the difference is primarily being made up by oxygen. One can deduce from the phase diagram of chromium and oxygen that Cr_2O_3 is primarily the oxide that exists between room temperature and 1,000°C. With this information in mind, an analysis was made of a pure iron whisker and a. whisker which substantially consisted of chromium.

Table III[(a)] shows the computer analysis results of a whisker that is almost entirely composed of iron; the calculations indicate a 1.6% Cr composition. The fit is very good and there is no reason to expect that significant amounts of any other elements are present. However, as the chromium content increases, the total weight-percent-analyzed figure drops continuously. Table III[(b)] shows the results of two analyses of what is essentially a chromium whisker with an iron core. The first analysis, for iron and chromium only, calculated 72% Cr and 3.1% Fe for a total of approximately 75% analyzed. The second analysis, assuming oxygen by difference, provided 75% Cr, 3.1% Fe, and 22% O. Then, as directed, the program assumed that all of the chromium was present in the oxide and calculated that 109% of the mass analyzed was Cr_2O_3. Obviously, this indicates that the chromium is not entirely

TABLE III[a]

Comparison Between X-Ray Analyses for Whiskers
Containing Different Amounts of Cr

Fit[0.00 -> 20.47]

6/26 Spec B 100 Secs CHISQD = 0.81

Drift Factor 1.000

Ref .S CR-K FE-K

ZAF Correction

Drift Factor 1.000

Iter 1

----	K	[Z]	[A]	[F]	[ZAF]	CONC
CR-K	0.022	0.995	1.016	0.730	0.739	0.016
FE-K	0.981	1.000	1.004	1.000	1.005	0.987

Total = 1.003

(a) Computer printout for an almost entirely iron whisker.

TABLE III[b]

Comparison Between X-Ray Analyses for Whiskers Containing Different Amounts of Cr

Fit [0.00 -> 20.47]

6/26 Spec 9 100 Secs CHISQD = 1.31

Drift Factor 1.000

Ref .S CR-K FE-K

ZAF Correction

Drift Factor 1.000

Iter 1

----	K	[Z]	[A]	[F]	[ZAF]	CONC
CR-K	0.723	0.999	1.000	0.994	0.995	0.721
FE-K	0.023	1.004	1.297	1.000	1.303	0.031

Total = 0.751

Ref .S CR-K FE-K

ZAF Correction

Drift Factor 1.000

Iter 2

----	K	[Z]	[A]	[F]	[ZAF]	CONC	
CR-K	0.723	1.045	0.994	0.995	1.034	0.748	
FE-K	0.023	1.050	1.233	1.000	1.295	0.031	
0 -K	0.049	0.892	4.965	0.999	4.431	0.221	D

Total = 1.000

Oxide Results
Cr_2O_3 1.093
Fe 0.030
Total = 1.124

[b] computer printout for a whisker being almost entirely chromium.

combined in the oxide. Another approach is to assume that all of the oxygen is present in the oxide. A calculation involving the respective atomic weights shows that if 22% of the total mass analyzed is oxygen, then 48% of the total mass analyzed must be chromium combined with the oxygen in Cr_2O_3. The calculated concentration of chromium in the analysis was 75%. Therefore, 27% of the total mass analyzed must be composed of chromium in ferrite or carbide, and 64% of the amount present is involved in the oxide. The total weight-percent-analyzed is then the sum of: 70% Cr_2O_3, 27% Cr, and 3.1% Fe. This is a total of approximately 100%.

This calculation supports the assumptions that in chromium whiskers oxygen composes most of the balance of the total mass present and that essentially all of the oxygen is present in the oxide. The continuous decrease in the fraction of the total mass analyzed resulting from iron and chromium compositions as the chromium content is increased, indicates that the incorporation of oxygen into the deposit is directly related to the deposition of chromium. In the low to moderate alloy compositions a chromium-rich surface layer of cubic magnetite is expected.

As added evidence that the oxygen believed present in the chromium-alloyed whiskers is not a result of oxidation during heat-treatment, the composition analysis result for a chromium whisker heat-treated at 800°C in ultra-high-purity hydrogen is also plotted in Figure 10.

The microstructure of Fe whiskers looked similar to that of whiskers produced in the Schladitz machine, i.e. ring-like structures centered around the core of the whiskers after etching with NITOL. Similar ring patterns were seen in whiskers alloyed with Cr.

The microstructures of Fe-C whiskers and Fe-Cr-C whiskers are very similar. Even at very high Cr content the grain size remains in the 8 nm - 30 nm range as is known from Fe-C whiskers.

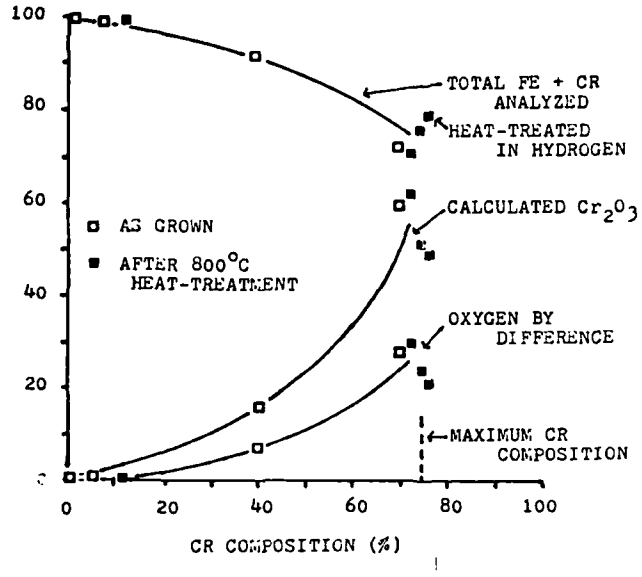

Figure 10. Relationship between the fraction of the total mass analyzed by energy-dispersive X-ray analysis and the chromium concentration in alloy whiskers. All ZAF corrections made assuming oxygen by difference.

Fe-Cr-C whiskers were annealed at 400°C, 600°C, and 800°C for 15 minutes in evacuated tubes. The structural changes during heat treatment were monitored by X-ray diffraction and by scanning electron microscopy. Observations by the latter showed that the etched cross-section of whiskers showed an increase of roundish small particles with increasing temperature and with increasing Cr content at each temperature. X-ray diffraction patterns revealed that drastic structural changes occurred during the three temperature treatments. At 400°C the pure metal ferrite phase and M_3C were present. At 600°C the ferrite phase and cementite were joined by Cr_2O_3. With increasing Cr content in the whiskers the first two phases were reduced while Cr_2O_3 increased. At 800°C the ferrite phase is present as well as M_3C and now α-M_3O_4 was also observed. SEM pictures showed etched surfaces of ferrite grains and pearlite. A 40% Cr filament showed a replacement of cemen-

tite by $(Cr,Fe)_7C_3$. Other structures in 40% Cr filaments are the ferrite phase and Cr_2O_3.

As expected, these structural changes affected the filaments' strength. A summary of the results of microhardness tests is given in Figure 11, based on average values. An addition of Cr to Fe-C whiskers reduces the microhardness somewhat. A 400°C heat treatment keeps the microhardness in the same range, namely between 700 and 1,000 Kg/mm^2 (~10GPa). 600°C and 800°C anneals reduce the microhardness of Fe-Cr-C whiskers to 500 Kg/mm^2 and 175 Kg/mm^2 respectively. After the 600°C anneal only 50% Cr containing whisker recovered their original strength but with increasing Cr content the microhardness went up to about 1,000 Kg/mm^2 (this is the strength of Fe-Cr whiskers as grown). Annealing at 800°C results in strength reduction below the 600°C anneal values for whiskers containing 5-50% Cr. However, the microhardness is increasing rapidly for 65-70% Cr containing whiskers to about 2,000 Kg/mm^2. A maximum value of 2,600 Kg/mm^2 has been recorded;

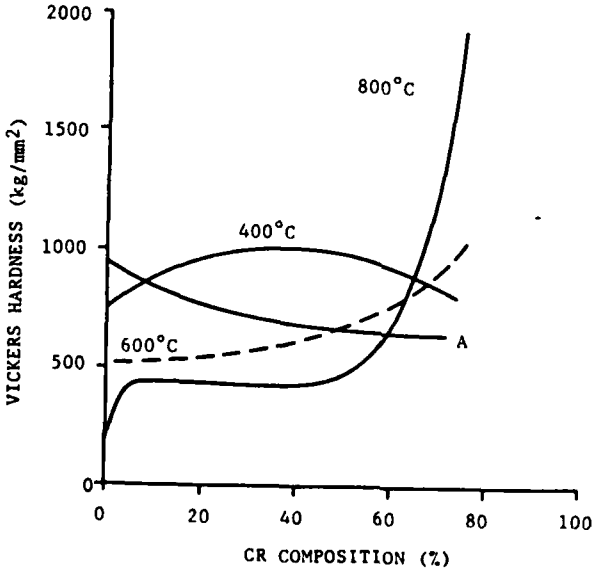

Figure 11. Microhardness as a function of composition for chromium-alloyed filaments heat-treated at 800°C. A = as grown.

this corresponds to a fracture strength of 8.6 GPa. Figure 12 summarizes the average microhardness vs. annealing temperature.

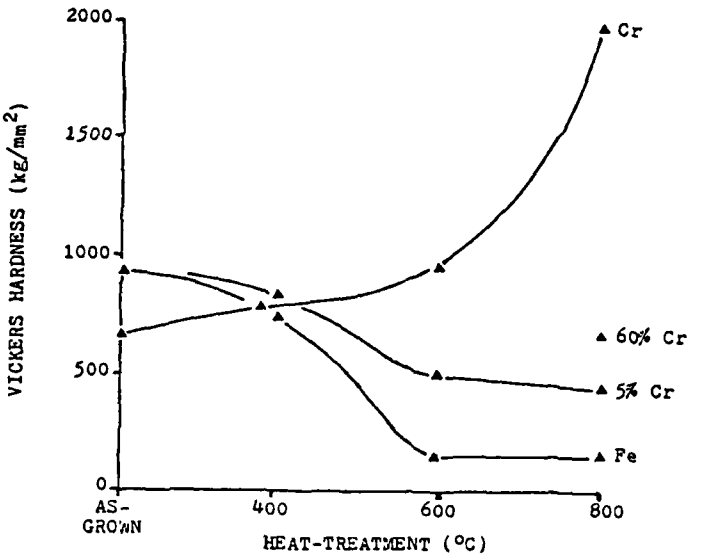

Figure 12. Microhardness vs. temperatures of heat-treatment for representative compositions.

The thermal decomposition of a mix of $Fe(CO)_5$ and $Cr(CO)_6$ vapors in a magnetic field led to the production of Cr containing Fe-C whiskers. The yield of one run provided whiskers from very low to very high Cr content in a reproducible fashion. Results from energy dispersive X-ray analyses showed that considerable amounts of oxides and carbides were incorporated into the whiskers, their amounts depending on the whiskers' Cr content. This growth behavior differs considerably from the growth mechanism of Fe-C whiskers; it is concluded that the decomposition of $Cr(CO)_6$ is accelerated by H_2 in comparison to the decomposition of $Fe(CO)_5$. An equally important factor is the reduction of the diffusion of carbon in α=Fe in the presence of Cr, leading to a different microstructure. These two conclusions are supported by independent reports in the literature.

Since the growth temperature was 250°C it is obvious that some of the phases must be in a metastable equilibrium. The heat treatments reported at 400°C, 600°C, and 800°C confirm this contention. With increasing temperatures Cr_2O_3 and $(Cr,Fe)_7C_3$ were seen by X-ray diffraction in whiskers containing high Cr contents. Naturally, this increased the microhardness in proportion to the percentage of the oxides and carbides. Practically then, the high Cr content whiskers were more like a ceramic substance than an alloy. This explanation is backed up by the hardness of Cr_2O_3 (2940 Kg/mm^2) and Cr_7C_3 (1136 Kg/mm^2) if taken in proper proportions and allowing that the rule of mixtures is applicable (the average microhardness for a chromium whisker after annealing at 800°C was approximately 2000 Kg/mm^2). However, 2.5% Cr containing Fe whiskers do not retain their original strength after an 800°C anneal as has been claimed in the literature. The error arose by determining the chemical composition from a large amount of whiskers* which, as has been demonstrated in our investigation, have varying amounts of Cr if prepared by mixing and decomposing $Cr(CO)_6$ and $Fe(CO)_5$ vapors.

* Personal Communication by H. Schladitz

SECTION III

CONCLUSIONS

Polycrystalline steel whiskers produced by a CVD technique in the presence of a magnetic field are to date the strongest polycrystalline alloys. Tensile strengths of up to 6 GPa have been measured at the University of Virginia by Lashmore (1977), and Schladitz (1968) reported values approaching 8 GPa. The structural details described in the previous chapter do not fit into any microstructural pattern known to exist in steels or, as a matter of fact, in any other alloys. The microstructure has been characterized through experimental findings as follows:

(i) Extremely small grain size (5 nm to 30 nm)

(ii) Lack of long range crystallinity within grains

(iii) Microdispersion of Fe_3O_4, Fe_3C, α-Fe_2O_3 and possibly carbon particles

(iv) Very diffuse grain boundaries

The four points made above have important implications in regard to the mechanical strengthening mechanism in the alloy. The most significant deviation of the CVD produced steel in comparison to alloys obtained by solidification is the lack of long range crystallinity as shown by field ion microscopy. On the other hand, α-Fe rings in electron diffraction patterns are composed largely of spots of varying sizes with some continuous intensity in the rings, i.e. both large and very small coherently diffracting volume elements consisting of α-Fe are present with particles of Fe_3O_4, Fe_3C, α-Fe_2O_3 and possibly carbon particles. The distribution of C remains obscure at this time, since only a small amount seems to be bonded to Fe as Fe_3C.

This investigation has clarified that the high strength of CVD steel whiskers is not due to the known strengthening mechanisms in alloys such as

solid solution hardening or second phase hardening. Instead, one has to conclude that the whiskers represent an assembly of particles of not more than 8 to 10 atomic diameters consisting of alpha-iron, iron oxides, iron carbides and carbon. Alpha-iron can be considered as the matrix holding the assembly together. It is indicated that the α-Fe grains are bonded together by multiple phase regions. On account of the nature of the growth conditions of this steel, it can be assumed that the very small particles in the microdispersion have concentration gradients which allows the conclusion that a mix of metallic bonds and covalent bonds exists in these transition regions that occupy possibly one-half of the whisker volume. The bond arrangement described would constitute the primary strengthening mechanism. The small grain size of the material and the absence of sharp grain boundaries provide for a more continuous microstructure largely free of the conventional interfaces present in solidified alloys. It is the combination of this feature combined with the specific bonding mix in transition regions which provide for the exceptional strength of this steel.

ACKNOWLEDGEMENT

The interest in this research shown by Dr. E. I. Salkovitz and Dr. B. MacDonald, Materials Division, Office of Naval Research, Arlington, Virginia, was a significant motivating influence to the principal investigator and his co-workers, and is gratefully acknowledged. Dr. MacDonald's scientific and technical understanding of high strength materials was of great help in planning and carrying out this research effort.

Professors L. E. Murr and O. T. Inal at the New Mexico Institute of Mining and Technology, and Professors W. L. Gettys and J. G. Stevens at the University of North Carolina, Asheville, have made substantial contributions through a field ion microscopy study and a Mössbauer investigation, respectively.

At the University of Virginia, I received much needed assistance from W. A. Jesser, D. Kuhlmann-Wilsdorf, D. M. Schladitz, H. J. Schladitz, and F. E. Wawner.

REFERENCES

1. C. Herring and J. K. Galt, Phys. Rev., 85, 1060 (1952).
2. S. S. Brenner, J. Appl. Phys., 27, 1484 (1956).
3. S. S. Brenner, J. Appl. Phys., 28, 1023 (1957).
4. E. Wolff and T. Coshren, J. Amer. Ceramic Soc., 48, 279 (1965).
5. S. Bokstein, S. Kishkin, and I. Svetlov, Soviet Physics - Solid State, 4, 1272 (1963).
6. R. Mehan, W. Sutton, and J. Herzog, AIAA Jour., 4, 1889 (1966).
7. F. R. N. Nabarro and P. J. Jackson, in Growth and Perfection of Crystals, Doremus, Roberts and Turnbull, Eds., John Wiley and Sons, New York, 1958, pp. 13-99.
8. L. Ercker, Treaties on Ores and Assaying (1574, 2nd ed. 1580), translated by A. G. Sisco and C. S. Smith, University of Chicago, 1951.
9. W. Dawihl and W. Eicke, Powder Metallurgy International, 3, 75 (1971).
10. H. J. Schladitz in Verbundwerkstoffe, Fachberichte, Tagung Konstanz 1972, Deutsche Gesellschaft für Metallkunde, 1972, pp. 153-169.
11. H. J. Schladitz, Zeitschrift f. Metallkunde, 59, 18 (1968).
12. H. J. Schladitz, Fachberichte für Oberflächentechnik, 8, 145 (1970).
13. H. J. Schladitz, Ingenieur Digest, 11, Heft 12 (1972).
14. W. Dawihl and W. Eicke, Berg- und Hüttenmännische Monatshefte, 116, 473 (1971).
15. H. E. Carlton and W. M. Goldberger, J. Metals, 17, 611 (1965).
16. D. S. Lashmore, Ph.D. Dissertation, University of Virginia, 1977.
17. J. W. Newkirk and H. G. F. Wilsdorf, to be published.
18. D. Tabor, J. Inst. Metals, 79, 1 (1951).
19. J. R. Cahoon, W. H. Broughton, and A. R. Kutzak, Metall. Trans., 2, 1979 (1971).
20. T. I. Ejim, M. S. Thesis, University of Virginia.
21. T. M. Moore, M. S. Thesis, University of Virginia, 1978.
22. H. G. F. Wilsdorf, O. T. Inal, and L. E. Murr, Z. Metallkd., 69, 701-705 (1978).

23. L. E. Murr and O. T. Inal, J. Appl. Phys., 42, 3387 (1971).

24. W. L. Gettys, J. G. Stevens, and H. G. F. Wilsdorf, Scripta Met., 13, 933 (1979).

25. H. G. F. Wilsdorf in Proceedings of the Fifth International Conference on the Strength of Metals and Alloys (Aachen, Germany) Vol. 1, P. Haasen, V. Gerold, and G. Kostorz, eds., Pergamon Press, New York, 1980, pp. 669-674.

26. L. E. Murr, Interfacial Phenomena in Metals and Alloys, Addison-Wesley, Reading, Massachusetts, 1975, pp. 192-218.

27. J. W. Newkirk, Ph.D. Dissertation, University of Virginia, 1982.

28. H. Fransen, H. Schladitz, and H. Borchers, Metall., 19, 423 (1965).

29. T. M. Moore, Ph.D. Dissertation, University of Virginia, 1980.

DISTRIBUTION LIST

Copy No.	
1 - 6	Office of Naval Research Department of the Navy 800 N. Quincy Street Arlington, VA 22217 Attention: Metallurgy Division Code 471
7 - 8	Mr. C. Richard Main Office of Naval Research Resident Representative 2110 G Street, N.W. Washington, D. C. 20037
9 - 10	H. G. F. Wilsdorf
11	K. R. Lawless
12 - 13	E. H. Pancake Sci/Tech. Information Center
14 - 92	ONR Distribution (Addresses Attached)
93	RLES Files

JO#2371:jt
Disk#263R

Defense Documentation Center
Cameron Station
Alexandria, VA 22314

Naval Air Propulsion Test Center
Trenton, NJ 08628

Attention: Library

Office of Naval Research
Department of the Navy
800 N. Quincy Street
Arlington, VA 22217

Attention: Code 471

Naval Construction Batallion
Civil Engineering Laboratory
Port Hueneme, CA 93043

Attention: Materials Division

Office of Naval Research
Department of the Navy
800 N. Quincy Street
Arlington, VA 22217

Attention: Code 102

Naval Electronics Laboratory
San Diego, CA 92152

Attention: Electron Materials
Sciences Division

Office of Naval Research
Department of the Navy
800 N. Quincy Street
Arlington, VA 22217

Attention: Code 470

Naval Missile Center
Materials Consultant
Code 3312-1
Point Mugu, CA 92041

Commanding Officer
Office of Naval Research
Branch Office
Building 114, Section D
666 Summer Street
Boston, MA 02210

Commanding Officer
Naval Surface Weapons Center
White Oak Laboratory
Silver Spring, MD 20910

Attention: Library

Commanding Officer
Office of Naval Research
Branch Office
536 South Clark Street
Chicago, IL 60605

David W. Taylor Naval Ship
Research and Development Center
Materials Department
Annapolis, MD 21402

Naval Undersea Center
San Diego, CA 92132
Attention: Library

Naval Research Laboratory
Washington, DC 20375
Attention: Code 6000

Naval Underwater System Center
Newport, RI 02840
Attention: Library

Naval Research Laboratory
Washington, DC 20375
Attention: Code 6100

Naval Weapons Center
China Lake, CA 93555
Attention: Library

Naval Research Laboratory
Washington, DC 20375
Attention: Code 6300

Naval Postgraduate School
Monterey, CA 93940
Attention: Mechanical Engineering
Department

Naval Research Laboratory
Washington, DC 20375
Attention: Code 6400

Naval Research Laboratory
Washington, DC 20375
Attention: Code 2627

Naval Air Development Center
Code 302
Warminster, PA 18964
Attention: Mr. F. S. Williams

NASA Headquarters
Washington, DC 20546
Attention: Code RRM

Naval Air Systems Command
Washington, DC 20360
Attention: Code 52031

Naval Air Systems Command
Washington, DC 20360
Attention: Code 52032

Naval Sea System Command
Washington, DC 20362
Attention: Code 035

NASA Lewis Research Center
21000 Brookpark Road
Cleveland, OH 44135
Attention: Library

Naval Facilities Engineering
Command
Alexandria, VA 22331
Attention: Code 03

National Bureau of Standards
Washington, DC 20234
Attention: Metallurgy Division

Scientific Advisor
Commandant of the Marine Corps
Washington, DC 20380

Attention: Code AX

Director Applied Physics Laboratory
University of Washington
1013 Northeast Fortieth Street
Seattle, WA 98105

Naval Ship Engineering Center
Department of the Navy
Washington, DC 20360

Attention: Code 6101

Defense Metals and Ceramics
Information Center
Battelle Memorial Institute
505 King Avenue
Columbus, OH 43201

Army Research Office
P.O. Box 12211
Triangle Park, NC 27709

Attention: Metallurgy & Ceramics Program

Metals and Ceramics Division
Oak Ridge National Laboratory
P.O. Box X
Oak Ridge, TN 37380

Army Materials and Mechanics
Research Center
Watertown, MA 02172

Attention: Research Programs Office

Los Alamos Scientific Laboratory
P.O. Box 1663
Los Alamos, NM 87544

Attention: Report Librarian

Air Force Office of Scientific
Research
Building 410
Bolling Air Force Base
Washington, DC 20332

Attention: Chemical Science Directorate

Argonne National Laboratory
Metallurgy Division
P.O. Box 229
Lemont, IL 60439

Air Force Materials Laboratory
Wright-Patterson Air Force Base
Dayton, OH 45433

Brookhaven National Laboratory
Technical Information Division
Upton, Long Island, NY 11973
Attention: Research Library

Library
Building 50, Room 134
Lawrence Radiation Laboratory
Berkeley, CA

Office of Naval Research
Branch Office
1030 East Green Street
Pasadena, CA 91106

Dr. T. R. Beck
Electrochemical Technology Corporation
10035 31st Avenue, NE
Seattle, Washington 98125

Professor R. H. Heidersbach
University of Rhode Island
Department of Ocean Engineering
Kingston, Rhode Island 02881

Professor I. M. Bernstein
Carnegie-Mellon University
Schenley Park
Pittsburgh, Pennsylvania 15213

Professor H. Herman
State University of New York
Material Sciences Division
Stony Brook, New York 11794

Professor H. K. Birnbaum
University of Illinois
Department of Metallurgy
Urbana, Illinois 61801

Professor J. P. Hirth
Ohio State University
Metallurgical Engineering
Columbus, Ohio 43210

Dr. J. A. S. Green
Martin Marietta Corporation
1450 South Rolling Road
Baltimore, Maryland 21227

Dr. Jeff Perkins
Naval Postgraduate School
Monterey, California 93940

Professor H. W. Pickering
Pennsylvania State University
Department of Material Sciences
University Park, Pennsylvania 16802

Professor R. W. Staehle
Ohio State University
Department of Metallurgical
Engineering
Columbus, Ohio 43210

Dr. E. A. Starke, Jr.
Georgia Institute of Technology
School of Chemical Engineering
Atlanta, Georgia 30332

Dr. R. P. Wei
Lehigh University
Institute for Fracture an
Solid Mechanics
Bethlehem, Pennsylvania 18015

Dr. William R. Prindle
National Academy of Sciences
National Research Council
2101 Constitution Avenue
Washington, DC 20418

National Bureau of Standards
Washington, DC 20234
Attention: Inorganic Materials Division

Air Force Office of Scientific
Research
Building 410
Bolling Air Force Base
Washington, DC 20332
Attention: Electronics & Solid State
Sciences Directorate

Dr. Otto Buck
Rockwell International
1049 Camino Dos Rios
P.O. Box 1085
Thousand Oaks, California 91360

Dr. D. W. Hoeppner
University of Missouri
College of Engineering
Columbia, Missouri 65201

Dr. David L. Davidson
Southwest Research Institute
8500 Culebra Road
P.O. Drawer 28510
San Antonio, Texas 78284

Dr. E. W. Johnson
Westinghouse Electric Corporation
Research and Development Center
1310 Beulah Road
Pittsburgh, Pennsylvania 15235

Dr. D. J. Duquette
Department of Metallurgical Engineering
Rensselaer Polytechnic Institute
Troy, New York 12181

Professor R. M. Latanision
Massachusetts Institute of Technology
77 Massachusetts Avenue
Room E19-702
Cambridge, Massachusetts 02139

Professor R. T. Foley
The American University
Department of Chemistry
Washington, D.C. 20016

Dr. F. Mansfeld
Rockwell International Science
Center
1049 Camino Dos Rios
P.O. Box 1085
Thousand Oaks, California 91360

Mr. G. A. Gehring
Ocean City Research Corporation
Tennessee Avenue & Beach Thorofare
Ocean City, New Jersey 08226

Professor A. E. Miller
University of Notre Dame
College of Engineering
Notre Dame, Indiana 46556

UNIVERSITY OF VIRGINIA
School of Engineering and Applied Science

The University of Virginia's School of Engineering and Applied Science has an undergraduate enrollment of approximately 1,450 students with a graduate enrollment of approximately 500. There are 125 faculty members, a majority of whom conduct research in addition to teaching.

Research is an integral part of the educational program and interests parallel academic specialties. These range from the classical engineering departments of Chemical, Civil, Electrical, and Mechanical and Aerospace to departments of Biomedical Engineering, Engineering Science and Systems, Materials Science, Nuclear Engineering and Engineering Physics, and Applied Mathematics and Computer Science. In addition to these departments, there are interdepartmental groups in the areas of Automatic Controls and Applied Mechanics. All departments offer the doctorate; the Biomedical and Materials Science Departments grant only graduate degrees.

The School of Engineering and Applied Science is an integral part of the University (approximately 1,500 full-time faculty with a total enrollment of about 16,000 full-time students), which also has professional schools of Architecture, Law, Medicine, Commerce, Business Administration, and Education. In addition, the College of Arts and Sciences houses departments of Mathematics, Physics, Chemistry and others relevant to the engineering research program. This University community provides opportunities for interdisciplinary work in pursuit of the basic goals of education, research, and public service.


ATE
LME